

DISCUSSION OF POSSIBLE EVIDENCE FOR NON-LINEAR BCS RESISTANCE IN SRF CAVITY DATA TO MODEL COMPARISON*

P. Bauer[#], N. Solyak, Fermilab, Batavia, USA
 G.L. Ciovati, TJNAF, Newport News, USA
 G. Ereemeev, Cornell University, Ithaca, USA
 A. Gurevich, University of Wisconsin, Madison, USA
 L. Lilje, DESY, Hamburg, Germany
 B. Visentin, CEA, Saclay, France

Abstract

Very powerful RF cavities are now being developed for future large-scale particle accelerators from high purity sheet niobium (Nb) superconductor. Today's advanced prototype resonator cavities operate in peak RF surface magnetic fields of up to 180 mT at quality factors $Q > 10^{10}$. This is the result of a successful worldwide technology development effort over the last decades.

The basic model for Q-slope in SRF cavities, i.e. the reduction of the cavity quality factor with increasing operating electric and magnetic fields, is the so-called thermal feedback model (TFBM). The exponential dependence of the BCS surface resistance $R_s(T)$ of the superconductor on the temperature T provides a positive feedback with the RF power dissipation ultimately leading to thermal runaway (thermal quench) of the RF exposed surface. Most important for the agreement between the model and experimental data, however, is which different surface resistance contributions are included in the TFBM calculation. This paper presents an attempt to further clarify if the non-linear pair-breaking correction to the BCS resistance [1,2] is among those essential surface resistance contributions, through a comparison of TFBM calculations with experimental data from bulk Nb cavities. The discussion encompasses a wide variety of cavities from DESY, CEA-Saclay, J-Lab, Cornell University and Fermilab.

THE THERMAL FEEDBACK MODEL

The small but finite amount of heat deposited on the inner surface of the superconducting RF cavity during operation is conducted through the cavity wall and into the liquid helium bath surrounding the cavity. In the TM01 mode the heat is mostly generated in a wide strip around the equator area, where the magnetic field (and thus the surface current) peaks. The peak field area is wide enough to allow for a one-dimensional representation of the thermal problem. The temperature profile across the Nb bulk and the temperature drop across the Nb-helium interface (with the cavities usually operating in superfluid helium the thermal impedance of the helium can be neglected) can be calculated exactly from the steady state heat balance equation and the temperature dependent thermal properties, thermal conductivity $\kappa(T)$ and Kapitza interface conductance h_{Kap} .

The thermal diffusivity of high purity, polycrystalline Nb at 2 K is of the order of 0.01 m²/sec, which, for mm thick walls, gives ~msec thermal equilibration times. RF pulses are typically of that length (or longer) and therefore the process is reasonably well described as a steady state.

The following briefly summarizes the thermal feedback model. A more detailed discussion can be found in [1]. We solve the following steady state heat balance equation

$$\frac{\partial}{\partial x} \kappa(T) \frac{\partial T}{\partial x} + P_{diss}(T_m, H_c, \dots) \delta(x) = 0 \quad (1)$$

$$P_{diss} = \frac{1}{2} R_s(T_m) H_{RF}^2 \quad (2)$$

which contains heat conduction and generation terms, where the delta-function in Eq. (1) reflects the fact that the RF heating is concentrated in a very thin surface layer of thickness $\lambda \sim 40$ nm, where λ is the London penetration depth. The RF power dissipated per unit area in the cavity depends on the RF magnetic field amplitude H_{RF} and the (temperature dependent) RF surface resistance $R_s(T)$ as given in Eq. (2). The equation assumes that the loss is due to the RF shielding currents only and neglects the contribution by electric surface fields (and associated dielectric loss for instance).

The solution of Eq. (1) depends on the surface temperatures on both sides of the Nb sheet. The temperature on the RF exposed side, T_m , drives the surface resistance, while the temperature on the helium side, T_s , drives the Kapitza interface conductance. They can be derived exactly from the boundary conditions (Eqs. 3 & 4) for a given H_{RF} , T_0 and $R_s(T_m, H_{RF}, \dots)$.

$$h_{Kap}(T_s, T_0) d(T_s - T_0) = \int_{T_s}^{T_m} \kappa(T') dT' \quad (3)$$

$$\frac{1}{2} R_s(T_m, H_c, \dots) H_{RF}^2 = h_{Kap}(T_s, T_0) (T_s - T_0) \quad (4)$$

In this work we will use the exact, numerical solutions of Eqs. (3)&(4), unlike simplified TFB-models which have been often used in the literature.

The strong temperature dependence of the BCS resistance is at the core of thermal feedback. The increase

*Supported by the U.S. Department of Energy

[#]pbauer@fnal.gov

of the surface resistance with field is the result of a feedback process during which the surface temperature increases due to RF heating, while the RF heating increases with surface temperature. The feedback is strong because of the exponential dependence of the BCS surface resistance on temperature. In this process the cavity surface temperature increases as the applied RF magnetic field increases until thermal run-away occurs. In the absence of other limitations (such as the critical magnetic field) the thermal model therefore could also predict the applied RF magnetic field at which the cavity quenches. The quench field due to thermal feedback is typically referred to as “thermal quench field” H_b (as opposed to the superconductor critical field, H_c). The TFBM is only as good as the surface resistance and thermal parameter models that are put in. We will discuss here one of these models, following the procedure outlined by A. Gurevich in [1,2].

RF SURFACE RESISTANCE

The RF surface resistance of bulk, high purity Nb in the superconducting state is very small but cannot be neglected. It is usually defined as a sum of the BCS resistance $R_{s,BCS}$, and the residual resistance R_{res} . Other contributions due to field enhancement on grain edges, trapped magnetic flux or vortex penetration in grain boundaries can also be added (a review of different surface resistance contributions can be found in [3]). The BCS RF surface resistance results from the interaction between the RF fields (localized in a surface layer defined by the London penetration depth λ) and the thermally activated electrons in the superconductor:

$$R_{s,BCS}^{lin}(T) = \frac{A(\omega^2, \Delta)}{T} e^{-\frac{\Delta}{k_b T}} \quad (5)$$

where $\Delta \sim 1.5 \text{ meV}$ is the superconducting energy gap, and the factor $A(\Delta, \lambda, \xi, \ell, T) \propto \omega^2$ depends on Δ , λ , the coherence length ξ_0 ($\sim \lambda_0$), and the mean free path ℓ [1]. The superconducting material parameters may vary strongly throughout λ due to the presence of metallic oxides and defects on the surface and along grain boundaries [4]. Therefore, in the absence of exact parameter profiles of the material in the cavities, the linear BCS surface resistance is typically written in the form of Eq. (5) with the understanding that the parameters $A(\omega)$ and Δ are actually averaged over λ .

Eq. (5) gives the linear BCS surface resistance, i.e. the BCS contribution at fields much lower than the critical field H_c . At RF fields approaching the critical field the coherent motion of the Cooper pairs constituting the shielding current causes a reduction of the effective gap in the quasiparticle spectrum, greatly increasing the density of thermally-activated electrons and thus the BCS loss. The non-linear BCS surface resistance for a type-II superconductor ($\lambda > \xi$) at low frequencies $h\omega \ll \Delta$ in the clean limit can be obtained in the form [2]:

$$R_{s,BCS}^{nlin}(T, B) = \frac{8R_{s,BCS}^{lin}(T)}{\pi\beta^2(T)h^2} \left[\int_0^\pi \sinh^2 \left[\frac{\beta(T)h}{2} \cos(t) \right] \tan^2(t) dt \right] \quad (6)$$

$$\beta(T) = \frac{\pi}{2^{3/2}} \frac{\Delta}{k_b T}, \quad h = \frac{H_{RF}}{H_{c,0}}$$

The integral can be solved analytically for small and large βh , where $h < 1$ is the reduced magnetic field. For low fields, $\beta h \ll 1$, the first nonlinear correction is quadratic in H_{RF} , while for high fields $\beta h \gg 1$, the non-linear BCS resistance increases exponentially:

$$R_{s,BCS}^{nlin1}(T, B) = R_{s,BCS}^{lin}(T) \left[1 + \frac{\beta^2}{48} \left(\frac{H_{RF}}{H_{c,0}} \right)^2 \right] \quad (7)$$

$$R_{s,BCS}^{nlin2}(T, B) = R_{s,BCS}^{lin}(T) \left[\frac{4e^{\beta(T) \frac{H_{RF}}{H_{c,0}}}}{\beta(T)^{7/2} \sqrt{2\pi}} \right] \left(\frac{H_{c,0}}{H_{RF}} \right)^{7/2} \quad (8)$$

The BCS resistance, which is strongly temperature dependent, can be derived from Q measurements in the cavity at different temperatures. The fit of the temperature dependence of the surface resistance allows us to separate temperature dependent (BCS) and independent (residual) surface resistance contributions. This procedure is easiest (and usually applied) at low field where it yields the linear BCS component. At high fields the low and high field BCS contributions need to be distinguished, adding difficulty to the procedure.

The non-linear BCS surface resistance is defined by Eq. (6) for the clean-limit ($\ell \gg \xi_0$) only. Taking into account of impurity scattering is a much more complicated problem, but a first order quadratic correction of the non-linear BCS resistance for arbitrary mean free path can be written in the form similar to Eq. (7):

$$R_{s,BCS}^{nlin}(T, B) = R_{s,BCS}^{lin}(T) \left[1 + C(\ell, \omega, T) \left(\frac{H_{RF}}{H_c} \right)^2 + \dots \right] \quad (9)$$

where $C(\ell, \omega, T)$ is now a function of the mean free path, and $H_c(T)$ is the thermodynamic critical field at operating temperature. In the clean limit C is of the order of unity in Nb at $\sim 2 \text{ K}$ and increases as the temperature decreases (see Eq. (7)). Note that the larger C becomes, the smaller the field range in which the first order expansion in Eq. (9) is valid. Generally, C decreases as ℓ decreases, that is, the BCS nonlinearity becomes less pronounced as the surface layer gets more contaminated with impurities. Given a very little information about the mean free path in the cavity surface layer, the value of C in Eq. (9) can be regarded as a fit parameter in the TFB calculations.

state of the art and have as little low and medium field Q -slope as possible, such as to limit the surface resistance to the basic residual and BCS components. The latter condition would obviously improve the model/data agreement, with the model using only BCS (and residual) resistance. All the cavity experimental results discussed here were chosen with these criteria in mind. For some cavities we had data both at ~ 2 K and ~ 4.2 K. Most cavities were single-cell prototypes, with the only exception being the DESY AC70, which is a full-length 9-cell TESLA cavity. The Saclay and DESY cavities were electro-polished, while the J-Lab, Cornell and FNAL cavities were BCP etched. The J-Lab cavities and the Saclay cavity C115 were also post-purified (heat treated at $\sim 1400^\circ\text{C}$ in the presence of Ti to increase RRR). The thermal conductivity function was not modified to account for the increased RRR. The data obtained before and after the low temperature bake ($\sim 120^\circ\text{C}$, 50 hrs) are presented. Essentially all Q measurements were performed in the CW (=steady state) mode.

The results of the data-model comparisons are shown in Figs 2-8. The figures typically show the cavity quality factor before and after baking as a function of peak magnetic field (at the equator). Typically three sets of model calculations, in at least one of the two cases, are shown as well (given in the order of increasing curvature at high field): -1- using the linear model (Eq. 5), -2- using the quadratic approximation of the model for general mean free path (Eq. 9) and -3- using the non-linear model in the clean limit (Eq. 6). In the 4.2 K cases only models 1) and 3) are shown. The different data-model comparisons need to be evaluated on a case-by-case basis. However, certain trends can be identified. The clean limit non-linear resistance model, which produces the strongest Q -slope at high field, predicts a steep Q -slope in the lowest temperature cases (before-baking), albeit at a field slightly higher than seen in the data. In the case of the CEA-C1-03 cavity the 4.2 K data further confirm that the surface resistance is BCS dominated with no evidence of abrupt kinks on $Q(H)$ curves indicative of vortex penetration either in the bulk or along networks of grain boundaries.. At 4.2 K the non-linear BCS contribution is almost entirely suppressed, which is consistent with Eq.6.

For ~ 2 K cases, the quality factor before and after baking is better described by Eq. (9) with $C \sim 1-4$ in the medium field region. The non-linear, clean limit model usually predicts a too strong slope. At 120 mT, before baking, however, a kink appears, followed by a strong Q -drop, which cannot be described with any model discussed here. In the Fermilab 3.9 GHz case there are no data for after baking. The before baking data are consistent with linear BCS resistance only.

An issue, which was reported in the context of the CU cavity EI1-30, is the possible increase of the bath temperature during the testing (50 mK in EI1-30). We calculated that in this case a bath temperature increase by 500 mK (at $h=1$, with $T \sim T_0(1 + h^2)$) is needed to explain the Q -drop in the after baking condition even after

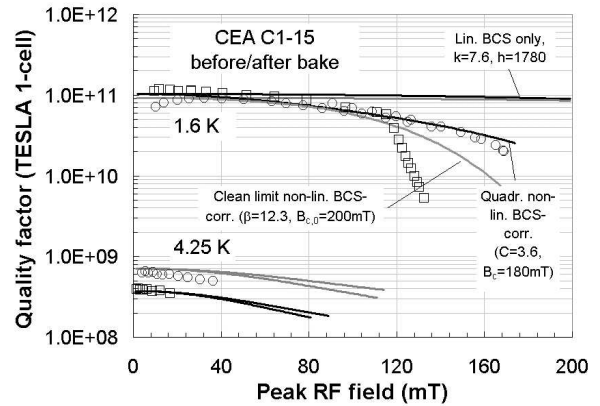


Figure 2: Comparison of measured and predicted quality factor of a CEA/Saclay single cell TESLA cavity (C-115) before and after baking. Experimental data were obtained at 1.6 K and 4.25 K. The cavity was electro-polished and post-purified and has a very small residual surface resistance.

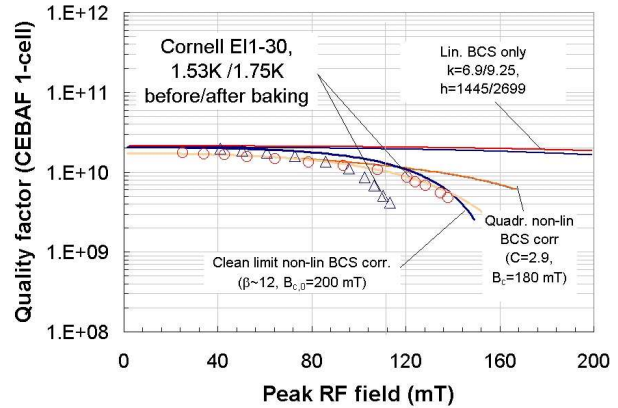


Figure 3: Comparison of measured and predicted quality factor of a Cornell University single cell CEBAF cavity (EI1-30) before and after baking. Experimental data were obtained at 1.53 K before and 1.75 K after baking. The bath temperature increased by ~ 50 mK during the test.

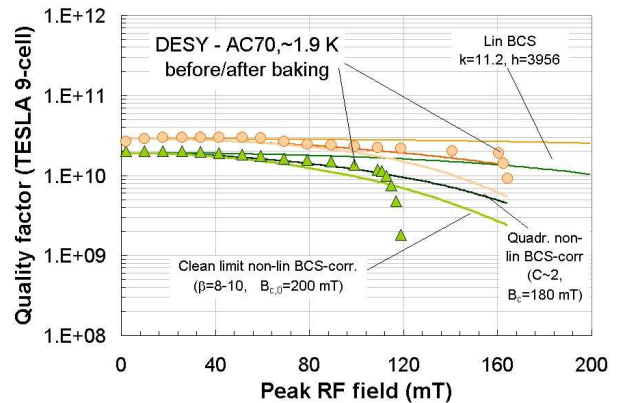


Figure 4: Comparison of measured and predicted quality factor of a DESY 9-cell TESLA cavity (AC70) before and after baking. Experimental data were obtained at ~ 1.9 K. The cavity was electro-polished.

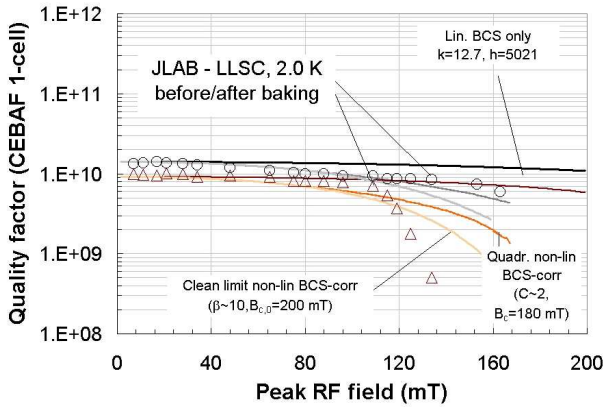


Figure 5: Comparison of measured and predicted quality factor of a JLAB low loss, single cell CEBAF cavity (LLSC, 1.5 GHz) before and after baking. Experimental data were obtained at 2.0 K.

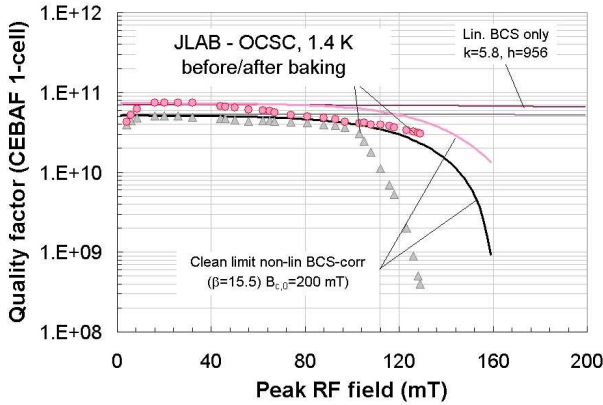


Figure 6: Comparison of measured and predicted quality factor of a JLAB single cell CEBAF cavity (OCSC – original CEBAF shape, 1.5 GHz) before and after baking. Experimental data were obtained at the very low temperature of 1.4 K, which explains the high Q.

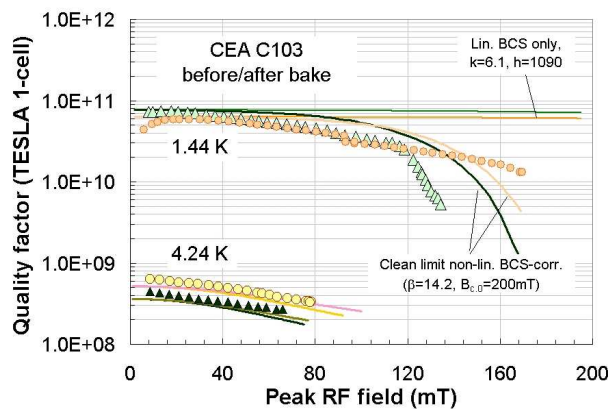


Figure 7: Comparison of measured and predicted quality factor of a CEA/Saclay single cell TESLA cavity (C 103) before and after baking. Experimental data were obtained at a very low (1.44 K) and high (4.2 K) temperature.

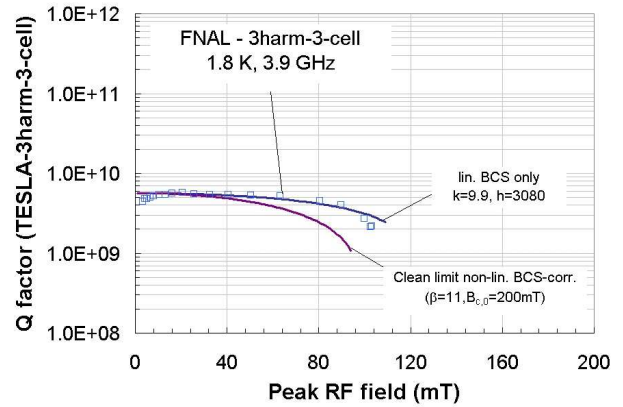


Figure 8: Comparison of measured quality factor of a Fermilab 3rd harmonic (3.9 GHz) 3-cell cavity to model predictions. Experimental data were obtained at 1.8 K. There are no after baking data.

including the quadratic non-linear BCS (Eq. 9) and residual resistance. Since this is much more than the observed temperature change, the effect was not considered any further in the calculations.

DISCUSSION

The data-model comparisons show that TFBMs based solely on the linear BCS and residual surface resistances (as measured at low field) strongly under-estimate the medium-field Q-slope in ~ 1.5 GHz cavities. This was already reported by several other authors [9]. If the nonisothermal low-field surface resistance is expressed in terms of the phenomenological parameter γ in $R_s(H) = R_{BCS}[1 + \gamma(H_{RF}/H_c)^2]$, the TFBM on the basis of the linear BCS predicts $\gamma \sim 0.25$, while the data after baking are better described by $\gamma \sim 1-4$. In the before baking cases this applies only to the medium field slope, while a very strong Q-drop at high fields would require $\gamma \sim 500$. The variation of thermal properties in a reasonable range ($\sim \pm$ factor 2) could not transform a “linear-model case” into a non-linear case. The addition of the non-linear BCS contribution [1,2], improves the data-model agreement significantly, especially in the medium field region and the after baking condition. We would also like to note that, apart from the exceptional case of the Fermilab 3.9 GHz cavities, the thermal quench fields H_b predicted by TFBM on the basis of linear BCS and residual resistance only, are by a factor ~ 2 larger than the actual quench fields (the graphs in the plots are not shown beyond the 200 mT range, however).

Beyond these general findings, however, a very fragmented picture emerges. In the very low temperature cases (EI1-30 before baking, OCSC, C-103), the clean-limit, non-linear model predicts a strong Q-slope, albeit at slightly higher fields than measured (Figs 3,6,7). The calculated onset field can be made to agree with the measured data thermal properties reduced by a factor 2. In the 2 K cases (e.g. C115, AC-70, LLSC, or Figs 2,4,5) the

Q-curves follow the prediction based on the non-linear BCS model in the medium field region until ~ 120 mT, when the Q suddenly drops severely. The clean limit non-linear model does not predict this Q-drop. Perhaps additional mechanisms, such as discussed recently by Halbritter (dissipation at grain boundaries, [4]), Gurevich ("hot spots model", [2]) and Ciovati ("kappa model", [11]) could explain this severe Q-drop. These models also could explain the discrepancy between calculated and measured Q-drop onset field in the $T < 1.6$ K cases. It is not clear why the 2 K cases (AC70, C115, LLSC) at high fields are not as consistent with the clean-limit non-linear BCS resistance as the three < 1.6 K cases. One could also argue that the non-linear model applies better to low temperature cases because of the strong increase of the non-linear BCS resistance at lower temperature. It could also indicate that the AC70, C115, LLSC cavities happen to have a dirtier surface than C1-03, OCSC, EI1-30, such that the non-linear resistance was reduced, at the expense, however, of vortex penetration or other Q-drop causing phenomena?

After baking, the ultimate Q-drop is strongly reduced in all cases, and the clean-limit non-linear model overestimates the high field surface resistance for the cases shown in Figs. 2,5,7 and 8, but describes data well for the cases in Figs. 3 and 6. Gurevich proposed a transition to the "dirty" limit induced by e.g. oxygen contamination, as a possible explanation for the baking effect [2]. This hypothesis is consistent with models of contamination of the first 100 nm during baking discussed by many authors (e.g. [5], [9], [10] and [11]). The non-linearity of the surface resistance is reduced in the dirty limit, and different degrees of clean-to-dirty limit surface transitions have to be expected. The low surface resistance in the dirty limit is also a candidate to explain the particularly flat high field Q ($\gamma \sim 0.1$) in the historic "defect-free" cavity built and tested by P. Kneisel and his collaborators [12]. This model requires, however, that the surface is in the clean condition before baking, which cannot be concluded unambiguously from this data-model comparison. Experimental data about the mean free path at the cavity surface in these cavities would be needed. Note that the observed reduction in linear BCS resistance with baking (which is believed to be the result of impurity contamination) alone, does not explain the elimination of the Q-drop (the after baking non-linear model curves in the plots take into account the change in linear BCS resistance but overestimate the resistance). The non-linear clean limit BCS model is also not consistent with the data for the FNAL 3.9 GHz cavity (Fig. 8). This confirms a trend already noted in [10] that at frequencies beyond 1.5 GHz, the experimental data are better described using *only* linear BCS resistance. The linear model-data agreement in the Fnal 3rd harmonic case goes as far as to predicting the right thermal quench field. This behaviour might indicate that this cavity surface was also in a dirty limit or the kinetics of quasiparticles in Nb at higher frequencies is more complicated than the quasistatic

pairbreaking, which results in Eq. (6). Another uncertainty comes from the unclear nature of the residual resistance R_{res} , in particular its frequency and field dependences. The above conclusions are obviously contingent upon the many assumptions made in the model (thermal parameters, critical field, etc). The effect of the thermal properties on the Q-slope, however, is weak (the effect is best seen in the thermal quench field, which is usually out of the experiment's reach because of the critical field or other limitations).

CONCLUSIONS

Calculations based on the TFBM were implemented and applied to the case of the state of the art SRF cavities from CEA, DESY, J-Lab, CU and FNAL. This comparison reveals that incorporation of the nonlinear BCS resistance into the TFBM significantly improves the agreement with observed Q(H) curves at medium fields (and sometimes at high fields as well).

The Q-slope prediction with the non-linear BCS resistance in the clean limit underestimates the ultimate Q-drop before baking. This indicates that other mechanisms like hot spots or/and grain boundaries could account for the higher Q slope.

The medium field Q-slope before baking and the medium & high field Q-slope after baking in cavities tested at 2 K is reasonable well described by the dirty limit non-linear BCS resistance.

The nonlinear quasistatic BCS resistance in the clean limit overestimates the observed surface resistance in most cases.

REFERENCES

- [1] A. Gurevich, Pushing the Limits of RF Superconductivity workshop, ANL, Sept 22-24 2004
- [2] A. Gurevich, this conference
- [3] P. Bauer et al., FNAL Tech Div Memo TD-04-014, http://www-td.fnal.gov/info/td_library.html, 12/2004
- [4] J. Halbritter, Proceedings of the 11th RFSCWS, Luebeck, Germany, 2003
- [5] S. Casalbuoni et al., Nuclear Instruments and Methods in Physics Research A 538 pp 45-64, 2005
- [6] F. Koechlin, B. Bonin, CEA internal note DAPNIA-SEA-96-01, Jan. 1996
- [7] H. Mittag, Cryogenics, Vol. 13, p. 94, 1973
- [8] S. Van Sciver, "Helium Cryogenics", Plenum Press NY 1986
- [9] B. Visentin, RFSCWS 2003, Luebeck, Germany, Sept. 2003 or G. Ciovati, Pushing the Limits workshop, ANL, Sept 22-24 2004
- [10] G. Ciovati, Journal of Appl. Phys. Vol. 96/3, Aug. 2004
- [11] G. Ciovati, this conference
- [12] P. Kneisel et al., Proceedings of the 7th RFSCWS, Orsay France, 1995